Experimental Characterization of Temperature-Dependent Microwave Noise of Discrete HEMTs: Drain Noise and Real-Space Transfer

Bekari Gabritchidze[#*], Kieran Cleary[#], Jacob Kooi[^], Iretomiwa Esho[$], Anthony C. Readhead[#], Austin J. Minnich[$]

[#]Cahill Radio Astronomy Lab, California Institute of Technology, USA

[^]NASA Jet Propulsion Laboratory, California Institute of Technology, USA

[*]Department of Physics, University of Crete, Greece

[$]Division of Engineering and Applied Science, California Institute of Technology, USA

aminnich@caltech.edu

2022 IEEE/MTT-S International Microwave Symposium - IMS 2022 | 978-1-6654-9613-1/22/$31.00 ©2022 IEEE | DOI: 10.1109/IMS37962.2022.9865505

***Abstract*— We report wafer characterization of the S-parameters and microwave noise temperature of discrete GaAs and GaN HEMTs over a temperature range of 20 – 300 K. The measured noise temperature (T_{50}) exhibits a dependence on physical temperature that is inconsistent with a constant drain temperature, with T_d for the GaAs and GaN devices changing from $\sim$ 2000 K and $\sim$ 2800 K at room temperature to $\sim$ 700 K and $\sim$ 1800 K at cryogenic temperatures, respectively. The observed temperature dependence is qualitatively consistent with that predicted from a theory of drain noise based on real-space transfer of electrons from the channel to the barrier.**

***Keywords*— HEMTs, microwave measurements, cryogenics, low-noise amplifiers, drain temperature, real-space transfer.**

I. Introduction

High electron mobility transistors (HEMTs) based on III-V semiconductors are widely used as cryogenic low noise amplifiers in scientific applications such as radio astronomy [1] and quantum computing [2] due to their unparalleled low noise performance. Therefore, understanding the physical origins of electronic noise in HEMTs and how to mitigate them is of importance. The Poszpieszalski model [3] describes the noise with a generator at the gate of temperature T_g and a generator at the drain with noise temperature T_d. T_g is typically interpreted as the physical temperature of the gate (T_{ph}) [4] but T_d is used as a fitting parameter that is around 1–2 orders of magnitude higher than the physical temperature. The physical mechanism behind T_d and its dependence on physical temperature remains a topic of debate [4], [5], [6]. The extent to which we can reduce the cryogenic noise of HEMT LNAs closer to the fundamental quantum limit depends on our ability to understand and minimize the contribution of T_d to the overall noise temperature.

In this paper, we report on-wafer measurements of the DC characteristics, S-parameters, and the noise temperature at generator impedance of 50 ohms (T_{50}) of discrete GaAs and GaN HEMTs over temperatures from 20 K to 300 K using a cryogenic probe station. We extract the small signal and noise model of the HEMTs at each physical temperature and various biases, yielding T_d at each condition. We find that the trend of T_{50} versus physical temperature is inconsistent with that expected if T_d is independent of temperature. This finding constrains the physical origin of drain noise in HEMTs.

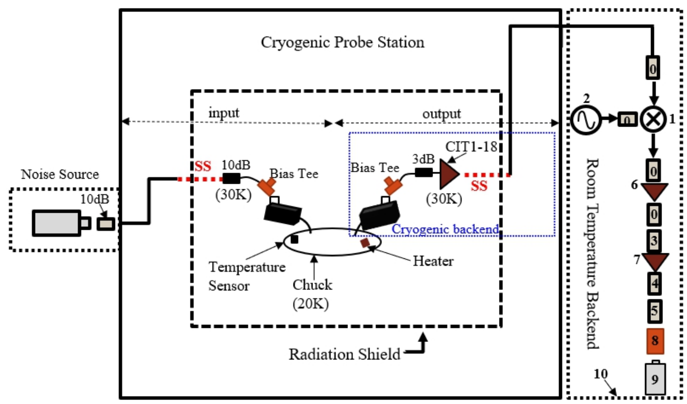

Fig. 1. Schematic of a cryogenic probe station configured for microwave noise measurements. The cryogenic and room temperature parts are separated by a radiation shield and stainless steel coaxial cables. (0) 5 dB pads, (1) M1-0220-P mixer, (2) HMC-T2100, (3) SLP-1000+ Low pass filter, (4) SLP-550+ Low pass filter, (5) SHP-25+ High pass filter, (6) ZFL-500LN+ Low noise amplifier, (7) ZFL-100H+ Low noise amplifier, (8) ZX73-2500-S Voltage-controlled attenuator, (9) U8481A USB thermocouple power sensor, (10) thermal insulation.

II. Cryogenic Characterization and Modelling

The DC characteristics, the S-parameters and the microwave noise of GaAs and GAN HEMTs were measured using a cryogenic probe station (CPS) [7]. A schematic of the cryogenic probe station in a noise-figure measurement configuration with a cryogenic attenuator is shown in Fig. 1. S-parameter and DC measurements require a simpler configuration in which the attenuators and the pre-amplifiers are removed. The CPS was configured to operate at variable sample-stage (chuck) temperature and at DC–40 GHz. A heater (Ohmite, TCH35 T0220) and a temperature sensor (Lakeshore, DT-470) were placed on the chuck to enable temperature control using a Lakeshore 336 temperature controller. The temperature uniformity of the chuck was measured to be within 1 K of the set temperature. Two devices were characterized: one GaAs (D007IH, 4F50, gate length L_g = 70 nm) and one GaN (D01GH, 2F50, L_g = 100 nm) HEMT, both manufactured by OMMIC (France). An image of a discrete GaAs HEMT contacted by RF probes is shown in Fig. 2.

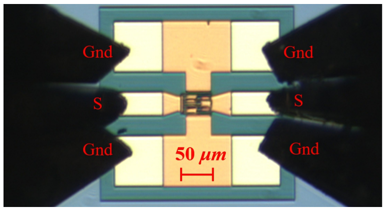

Fig. 2. Microscope image of RF probes landed on a GaAs discrete HEMT. The HEMT is in common source configuration. The source is grounded though the Gnd pins of the probes while signal is provided via the S pins to the gate (left) and drain (right).

A. HEMT Characterization

The S-parameters and DC characteristics of the HEMTs were measured at temperatures 20–300 K. Fig. 3 and Fig. 4 show the IV curves and S-parameters for the two devices at 40 K, 80 K, 150 K, and 296 K. V_{GS} was kept constant at -0.2 V and -1.2 V for the GaAs and GaN HEMT, respectively. At a given V_{DS}, the drain current is observed to increase with increasing temperature from 40 K to 300 K, consistent with the observed decrease in threshold voltage with increasing temperature (-0.23 V to -0.32 V for GaAs and -1.25 V to -1.38 V for GaN from 40 K to 300 K). In Fig. 4 the S-parameters are plotted at a constant DC bias of $V_{DS} = 0.6$ V, $I_{DS} = 10$ mA for the GaAs HEMT and V_{DS} =1.5 V, I_{DS} =10 mA for the GaN HEMT. A weak temperature dependence of S-parameters on physical temperature is observed.

The microwave noise temperature (T_{50}) was measured in the range 3-16 GHz using the Y-factor method with a cryogenic attenuator [8]. At each temperature, T_{50} was measured for $V_{ds} = 0.4$ V, 0.6 V, and 0.8 V for the GaAs and 0.5 V, 1.0 V, and 1.5 V for the GaN HEMT. For each V_{DS}, I_{DS} was varied from 5 mA to 20 mA by adjusting V_{gs}. Fig. 5 shows the frequency dependence of T_{50} at various physical temperatures and constant $V_{ds} = 0.6$ V, I_{DS} =10 mA for GaAs (a) and $V_{ds} = 1.5$ V, I_{DS} =10 mA for GaN (b). In Fig. 6, T_{50} versus I_{DS} is shown for various temperatures with constant $V_{DS} = 0.6$ V for GaAs and 1.5 V for GaN, at 12 GHz. The dominant contribution to the total uncertainty in T_{50} was found to be that of the insertion loss (IL), ~ 0.1 dB, in the path from noise source to the device. These uncertainties, in addition to the power-meter uncertainty, were propagated through the computation of the Y-factor to determine δT_{50}.

B. Cryogenic Modelling

A fifteen element small-signal model (SSM) identical to that described in [9] was extracted at each temperature and bias. The extrinsic parasitic elements and the intrinsic device elements were extracted based on cold FET measurements and direct extraction as described in [9], [10], [11]. The above intrinsic values were used as the initial values for the following tuning and optimization. These parameters were tuned in Keysight Advance Design System (ADS) to decrease the residual between the simulated and measured S-parameters. Additionally, simulated annealing, quasi-Newton optimization and the least-square error function were used to further

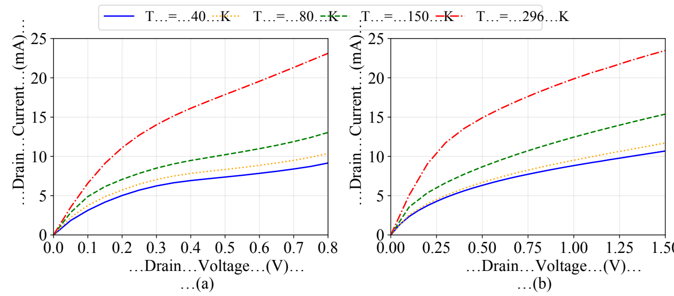

Fig. 3. Measured I-V curves at constant V_{gs} of (a) -0.2 V for GaAs and (b) -1.2 V for GaN at various physical temperatures.

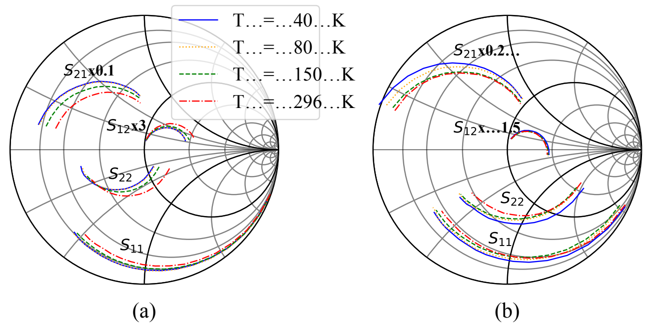

Fig. 4. Measured S-parameters at $V_{DS} = 0.6$ V, I_{DS} =10 mA for (a) GaAs and $V_{DS} = 1.5$ V, I_{DS} =10 mA (b) GaN HEMTs from 1-18 GHz at various physical temperatures.

decrease the residual to less than 0.01 dB. Both the tuning and optimization were restricted to within 10% of the initial values, and the specific values do not alter the findings regarding the microwave noise figure. Typical 40 K small signal conductances g_m and g_{ds} were ~ 850 mS/mm and ~ 95 mS/mm for GaAs; and ~ 670 mS/mm and ~ 50 mS/mm for GaN, respectively.

Once the SSM parameters were obtained, the noise model was generated automatically in ADS by ascribing a thermal noise source to the resistive elements. The gate temperature, T_g, was fixed to T_{ph}, while the drain temperature, T_d, was determined by fitting the modeled and measured T_{50}. Fig. 7 shows the extracted T_d versus I_{DS} and physical temperature at constant $V_{DS} = 0.6$ V and $V_{DS} = 1.5$ V, respectively. The error bars for T_d were determined by calculating T_d for the minimum and maximum values of T_{50} within the error bars and were found to range from $\sim \pm 150$ K to $\sim \pm 400$ K depending on physical temperature and δT_{50}. We observe a linear dependence of T_d on I_{DS} in this bias regime for both GaAs and GaN devices. This trend is consistent with those reported previously [2], [4]. The predicted T_{min} was calculated to be ~ 2.5 K for GaAs and ~ 15 K for GaN at 12 GHz.

III. Dependence of Drain Temperature on Physical Temperature

Fig. 8 shows the measured T_{50} versus physical temperature at 12 GHz and $V_{DS} = 0.6$ V, $I_{DS} = 10$ mA for GaAs

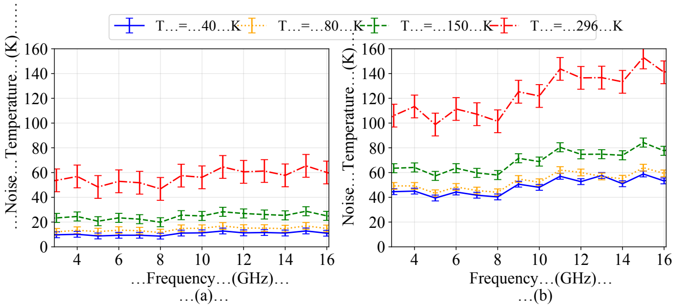

Fig. 5. T_{50} versus frequency at various physical temperatures and constant V_{DS} = 0.6 V, I_{DS} =10 mA for (a) GaAs and V_{DS} =1.5 V, I_{DS} =10 mA for (b) GaN.

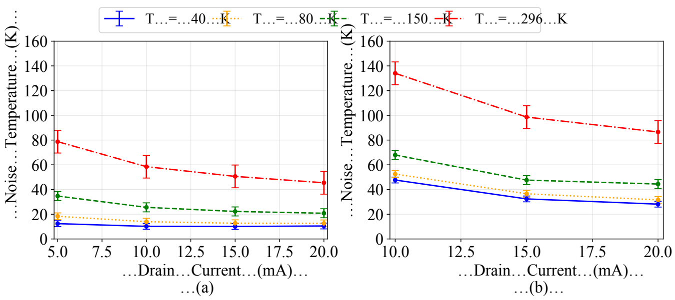

Fig. 6. T_{50} versus I_{DS} at V_{DS} = 0.6 V for (a) GaAs and V_{DS} =1.5 V for (b) GaN at various physical temperatures and constant frequency of 12 GHz.

and V_{DS} = 1.5 V, I_{DS} = 10 mA for GaN. Two GaAs devices from the same reticle were measured and yielded near-identical results. In addition, the predicted T_{50} versus physical temperature using the extracted SSM assuming T_d is fixed at its room temperature value is shown. The simulated and measured noise temperature are observed to decrease with decreasing T_{ph} for both devices, but the simulations predict a weaker trend with T_{ph} than the measurements.

The discrepancy between the measured and predicted T_{50} can be explained if T_d depends on physical temperature. The extracted T_d versus T_{ph} is shown in Figs. 8c and 8d. The T_d for both devices decreases with temperature, but the trend for the GaAs HEMT is more pronounced compared to that of the GaN HEMT. A dependence of T_d on physical temperature has been reported previously [9], [12]. However, a systematic study of T_d across a wide range of temperatures, biases, and III-V materials has not been reported, making it difficult to interpret the origin of drain noise in terms of a physics-based mechanism.

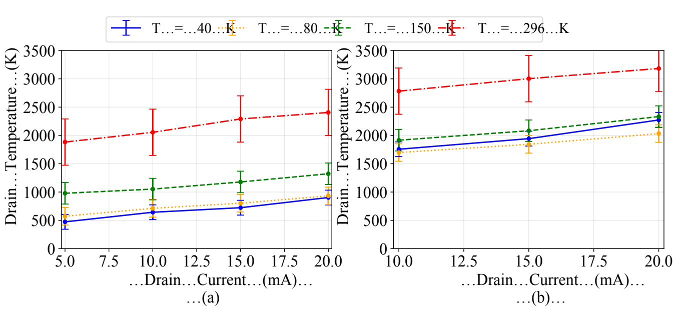

Fig. 7. Drain temperature T_d versus I_{DS} at constant V_{DS} = 0.6 V for (a) GaAs and V_{DS} = 1.5 V for (b) GaN at various physical temperatures.

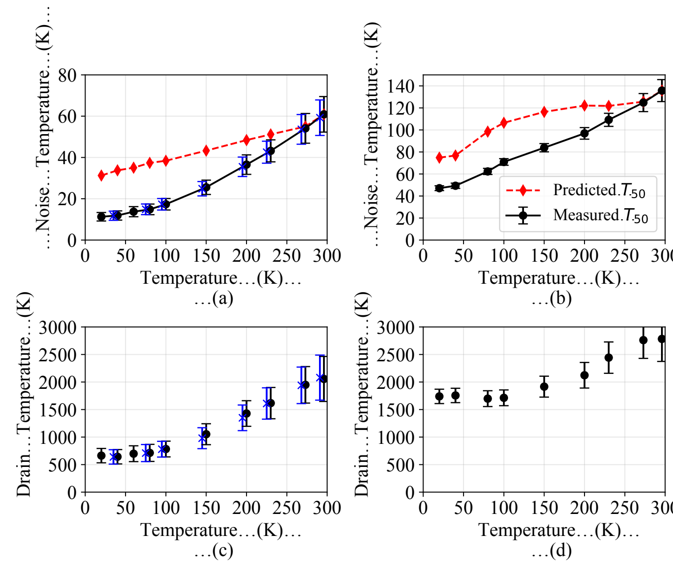

Fig. 8. Measured T_{50} versus physical temperature T_{ph} (circular marker and solid line) and predicted T_{50} versus T_{ph} using extracted SSM at each T_{ph} and assuming constant T_d at the 300 K value (red diamonds and dashed line) for (a) GaAs and (b) GaN HEMTs. Fitted T_d from measured T_{50} versus T_{ph} for (c) GaAs and (d) GaN. The V_{DS} and I_{DS} were fixed at V_{DS} =0.6 V and I_{DS} =10 mA in (a), (c) and at 1.5 V and 10 mA in (b), (d). In (a) and (c), T_{50} and T_d versus T_{ph} are shown for an additional GaAs device from the same wafer reticle (blue crosses). One data set was shifted to the left by 5 K to make the two data sets discernible.

Recently, a theory of drain noise based on real-space transfer of electrons from the channel to the barrier was reported [5]. In this theory, drain noise is a type of partition noise owing to the dissimilar mobilities of the channel and barrier. Because physical temperature affects the number of electrons that are energetic enough to thermionically emit into the barrier, the theory predicts T_d may exhibit a temperature dependence as shown in Fig. 3 of [5]. Comparing that figure and Fig. 8, we observe qualitative agreement, suggesting that the measured T_d versus T_{ph} is compatible with this theory of drain noise. The weaker dependence of T_d for the GaN device could also be accounted for in this theory as GaN heterojunctions exhibit a larger conduction band offset that thus inhibits real-space transfer processes. A more quantitative comparison is the topic of future work.

IV. Conclusion

We have measured the on-wafer I-V characteristics, S parameters, and microwave noise temperature of discrete GaAs and GaN HEMTs using a cryogenic probe station. The drain temperature exhibits a dependence on physical temperature, decreasing from $\sim 2000 \pm 400$ K to $\sim 700 \pm 150$ K and from $\sim 2800 \pm 400$ K to $\sim 1800 \pm 150$ K for the GaAs and GaN HEMT, respectively. These trends are qualitatively consistent with the physical origin of drain noise as arising from real-space transfer of electrons from the channel to the barrier.

Acknowledgments

The authors thank Sander Weinreb, Pekka Kangaslahti, James Lamb, Shi Jun, Junjie Li and Jan Grahn for useful discussions. This work was supported by the National Science Foundation under Grant No. 1911220.

References

[1] E. Bryerton, M. Morgan, and M. Pospieszalski, “Ultra low noise cryogenic amplifiers for radio astronomy,” in *2013 IEEE Radio and Wireless Symposium*, Jan. 2013, pp. 358–360.

[2] E. Cha, N. Wadefalk, G. Moschetti, A. Pourkabirian, J. Stenarson, and J. Grahn, “A 300-μw cryogenic hemt lna for quantum computing,” in *2020 IEEE/MTT-S International Microwave Symposium (IMS)*, Aug. 2020, pp. 358–360.

[3] M. Pospieszalski, “Modeling of noise parameters of mesfets and modfets and their frequency and temperature dependence,” *IEEE Transactions on Microwave Theory and Techniques*, vol. 37, no. 9, pp. 1340–1350, 1989.

[4] M.Pospieszalski, “On the dependence of fet noise model parameters on ambient temperature,” in *2017 IEEE Radio and Wireless Symposium (RWS)*, Jul. 2017, pp. 159–161.

[5] I. Esho, A. Y. Choi, and A. J. Minnich, “Theory of drain noise in high electron mobility transistors based on real-space transfer,” vol. 131, no. 8, p. 085111, publisher: American Institute of Physics. [Online]. Available: https://aip.scitation.org/doi/10.1063/5.0069352

[6] H. Felix, T. Fabian, L. Arnulf, and A. Oliver, “Noise performance of sub-100-nm metamorphic hemt technologies,” in *2020 IEEE/MTT-S International Microwave Symposium (IMS)*, Jul. 2020, pp. 293–296.

[7] D. Russell, K. Cleary, and R. Reeves, “Cryogenic probe station for on-wafer characterization of electrical devices,” *Review of Scientific Instruments*, vol. 83, no. 4, p. 044703, 2012.

[8] J. Fernandez, “A noise temperature measurement system using a cryogenic attenuator,” *TMO Progress Report*, no. 42, p. 135, 1998.

[9] M. Murti, J. Laskar, S. Nuttinck, S. Yoo, A. Raghavan, J. Bergman, J. Bautista, R. Lai, R. Grundbacher, M. Barsky, P. Chin, and P. Liu, “Temperature-dependent small-signal and noise parameter measurements and modeling on inp hemts,” *IEEE Transactions on Microwave Theory and Techniques*, vol. 48, no. 12, pp. 2579–2587, 2000.

[10] G. Dambrine, A. Cappy, F. Heliodore, and E. Playez, “A new method for determining the fet small-signal equivalent circuit,” *IEEE Transactions on Microwave Theory and Techniques*, vol. 36, no. 7, pp. 1151–1159, 1988.

[11] G. Kompa, *Parameter Extraction and Complex Nonlinear Models*. Norwood MA: Artech House, 2020.

[12] W. Sander and S. Jun, “Low noise amplifier with 7-k noise at 1.4 ghz and 25 °c,” *IEEE Transactions on Microwave Theory and Techniques*, vol. 69, no. 4, pp. 2345–2351, 2021.